

Trial to trial variability in either stimulus or action causes apparent correlation and synchrony in neuronal activity

Yoram Ben-Shaul^{a,*}, Hagai Bergman^a, Ya'acov Ritov^b, Moshe Abeles^a

^a Center for Neural Computation and The Department of Physiology, The Hebrew University, PO Box 12272, 91120 Jerusalem, Israel

^b Department of Statistics, The Hebrew University, Jerusalem, Israel

Received 19 January 2001; received in revised form 16 May 2001; accepted 18 May 2001

Abstract

In this report we show that the observed inter-neuronal correlation reflects a superposition of correlations associated with the intrinsic correlation between neurons, and correlations associated with variability in the stimuli presented to, or the actions performed by, the subject. We argue that the effects of either stimulus or action variability on the observed correlation, though generally ignored, can be substantial. Specifically, we demonstrate how observed correlations are effected by trial to trial variability in either stimulus or action. In addition, assuming that all relevant stimuli and actions are known, we outline a method for eliminating their effects on the observed correlation. It is also shown that tuning of correlations to a stimulus or an action might be a direct consequence of variability in that stimulus or action, even in the absence of any modulation of direct inter-neuronal interaction. The effects of stimulus and action variability should therefore be carefully considered when designing and interpreting experiments involving multi-neuronal recordings. © 2001 Elsevier Science B.V. All rights reserved.

Keywords: Correlation; Synchronization; Stimulus variability; JPSTH

1. Introduction

One of the most appealing notions concerning neuronal organization is that the *functional connectivity* between neurons is not fixed, but rather is a property of the state of the neuronal-network (Hebb, 1949; Gerstein et al., 1978, 1989; Abeles, 1982; Barlow, 1992; Nicolelis et al., 1997). The state of the neuronal-network is assumed to be related to the 'external world', defined in this context as the set of stimuli and actions perceived and performed by a subject¹.

If, as suggested above, the state of the neuronal network reflects the stimulus, then different patterns of stimuli should induce different patterns of interactions. Indeed, stimulus related interactions on various time

scales have been reported by several groups (Vaadia et al., 1991, 1995; Gruen, 1996; Hatsopoulos et al., 1998; Steinmetz et al., 2000; Baker et al., 2001). Some of these studies describe changes in correlation as a function of the stimulus or the behavioral set. Alternatively, the focus may be on the temporal modulation of the correlation (Aertsen et al., 1989; Ito and Tsuji, 2000). In the present report we argue that trial to trial stimulus variability can account for stimulus, or set dependent correlations. Alternatively, changes in stimulus variability as a function of time within a specific type of trial can lead to temporal modulations of correlation. These correlations are simply a consequence of a confounding variable, namely, the stimulus.

While the common experimental design of trial repetition assumes that all trials are identical, this condition is not always met. In fact, stimulus variability is not as rare as it may appear. When comparing controlled epochs (e.g. fixation on a visual target) to non-controlled epochs (e.g. no restriction on eye position), the differences in stimulus variability are obvious. However, stimulus variability also plays a role in 'controlled'

* Corresponding author. Tel: +972-2-6758384; fax: +972-2-6439736.

E-mail address: ybss@md2.huji.ac.il (Y. Ben-Shaul).

¹ Hereafter, to simplify the presentation, we shall use the term stimulus to represent either stimuli or actions or any combination of these.

situations. For example, fixation on a visual target does not ensure a constant visual input since micro saccades can still occur (Gur et al., 1997). Similarly, a ‘straight hand movement’ is rarely perfectly straight, and movements toward certain directions are often performed with larger variability as compared to other directions (Turner et al., 1995).

In the following sections we demonstrate and quantify the effects of stimulus variability on the observed correlation and synchrony between neurons. In the context of stimulus variability, we view spike count correlations (on a long time scale) and spike timing synchrony, as manifestations of the same phenomenon in different temporal scales. However, as these two cases call for a different mathematical analysis, they are treated separately.

2. Methods

2.1. Spike count distributions and their correlations

In our analysis, we assume that an experiment consists of a set of trials, where a trial is composed of a stimulus presented to the subject, an action performed by the subject, or any combination of stimuli and actions. As trials are performed, spikes emitted by (at least) two neurons are simultaneously recorded. Let $X_{i,[t,t+\Delta t]}(s_j)$ denote the number of spikes generated by neuron i , within a time interval $[t,t+\Delta t]$, in response to stimulus s_j . Here, s_j is the value of the stimulus in trial j , and t denotes the time relative to trial onset. The interaction between neurons, say $i=1$ and 2 , is measured by the correlation between $X_{1,[t,t+\Delta t]}(s_j)$ and $X_{2,[t,t+\Delta t]}(s_j)$, over the trial index j . In the context of this paper, we limit ourselves to the case of identical time segments for both neurons’ counts. In other words, our analysis deals with zero lag correlation. To simplify notation, we omit the trial index j , and the time specification $[t,t+\Delta t]$, and use $X_i(s)$ to denote the random variable representing the number of spikes generated by neuron i in response to stimulus s .

2.1.1. High spike count

We express the random variable $X_i(s)$, as a sum of a deterministic term $\mu_i(s)$, and a probabilistic noise term $N_i(s)$:

$$X_i(s) = \mu_i(s) + N_i(s) \quad (1)$$

In this formulation, both the mean response and the noise distribution are stimulus dependent. While expression (1) could in principle describe any random variable, we shall use it exclusively for spike count distributions in which $X_i(s)$ assumes values larger than 1.

To derive an explicit expression for the correlation between the spike counts of different neurons under various conditions (Section 3.2) we shall assume that the noise $N_i(s)$ is given by:

$$N_i(s) = \sigma_i(s)\tilde{N}_i = k_i\mu_i(s)^{m_i}\tilde{N}_i \quad (2)$$

where k_i and m_i are constants characteristic of neuron i , and \tilde{N}_i is a random variable with a mean of 0 and standard deviation (SD) of 1. We call \tilde{N}_i the *normalized noise*. Two assumptions are embodied in expression (2). The first equality implies that the noise distribution is given by a stimulus independent distribution (i.e. the distribution of \tilde{N}_i), scaled by a stimulus dependent standard deviation $\sigma_i(s)$. The second equality provides a rather general power law representation of $\sigma_i(s)$ as a function of $\mu_i(s)$. Such a power law relation between $\mu_i(s)$ and $\sigma_i(s)$ has been observed in various experimental studies (Gur et al., 1997; Lee et al., 1998). In particular, the special cases $m_i=0$ and $m_i=1$ correspond to spike count distributions in which the standard deviation is independent of the mean, or is a linear function of the mean, respectively. For $m_i=0.5$, it is the variance which varies linearly with the mean, in which case k_i is actually the square root of the Fano factor (Rieke et al., 1997).

To model the interaction between the neurons, we shall sometimes make the additional assumption that the normalized noise factors of a pair of neurons (\tilde{N}_1 and \tilde{N}_2), are derived from a bi-normal joint probability distribution with both means equal to 0, both standard deviations equal to 1, and a correlation coefficient ρ . Thus, ρ provides a measure for the interaction between the neurons. Under these assumptions, $X_i(s)$ is distributed normally with mean $\mu_i(s)$ and a standard deviation $\sigma_i(s)$. We shall therefore refer to this representation as the *normal approximation*. Note that, in general, $\rho = \rho(s)$, may depend on s , the specific value of the stimulus s .

Hereafter we shall refer to the correlations between the spike counts $X_i(s)$ as the *spike count correlations*. When the stimulus is kept constant across all trial repetitions (i.e. no stimulus variability), the correlation between the spike counts $X_i(s)$ of two neurons, as well as between the $N_i(s)$ and between the \tilde{N}_i factors, are identical. We name this correlation the *intrinsic correlation (IC)*, and regard it as a measure of the *functional connectivity* between neurons.

2.1.2. Low spike count

In the low count limit the firing of neuron i within a given time bin $[t,t+\Delta t]$ is modeled as a zero/one process with $P_i(s_j)$ denoting the spiking probability in the given time interval in response to s_j , the stimulus in trial j . In other words, the spike counts $X_i(s_j)$ in the interval $[t,t+\Delta t]$ follow a Bernoulli distribution with a success probability $P_i(s_j)$. Note that, in general, the success

probability is a function of the stimulus. If, however, the stimuli, and thus the firing probability, in all n trials are constant ($P_i(s_j) = P_i(s) = P_i$), then the sum of counts of neuron i over all n trials in a given time bin $[t, t + \Delta t]$ is distributed binomial: $\sum X_{i,t,t+\Delta t}(s_j) \sim b(P_i, N)$, where the sum is over the trial index j . Hereafter we omit the time interval specification and trial index.

Unlike in the high count case where the inter-neuronal interaction was quantified by the correlation coefficient, here we shall use the degree of *coincident spiking* as a measure of this interaction. We define the random variable Z as the number of trials in which both neurons spiked in the given time bin, summed over all n trials,

$$Z = \sum_j X_1(s_j)X_2(s_j). \quad (3)$$

If the firing probabilities of both neurons are independent and constant over all trial repetitions, then the probability that both neurons fire in the same time bin is given by the product P_1P_2 . Under these conditions, Z is also distributed binomial: $Z \sim b(P_1P_2, N)$ (Palm et al., 1988).

2.2. Estimation of spike count distributions

In the high count case, the spike count distribution is specified by the mean response $\mu(s)$, and the corresponding standard deviation $\sigma(s)$. In the low count case, where spike counts follow a Bernoulli distribution, only one parameter, the firing probability $P(s)$, is required. Next, we show how these parameters could be evaluated from the observed spikes counts and stimulus values.

2.2.1. High spike count

Our procedure for evaluating the function $\mu_i(s)$ from a set of stimulus values, and a corresponding set of spike counts, is illustrated in Fig. 1A. To obtain $\mu_i(s)$ we fit polynomials of various orders (typically 2–10) to an arbitrary half of the data set. The polynomials thus obtained are then used to approximate the responses $X_i(s)$ to the stimuli in the second half of the data. The polynomial order providing the best fit to the second part of the data set is subsequently used for evaluating $\mu_i(s)$ based on the entire data set. The purpose of this procedure is to find the highest polynomial order which does not result in over-fitting. The noise $N_i(s)$ in any trial associated with stimulus s , is obtained simply by subtracting the mean response $\mu_i(s)$ from the observed spike count $X_i(s)$.

Derivation of k_i and m_i (and hence $\sigma_i(s)$) from a set of stimulus values s , and a corresponding set of spike counts $X_i(s)$, is illustrated in Fig. 1B. First, the entire stimulus range (of the given data set) is divided into a

number of consecutive stimulus value bins. Then, the standard deviations of the counts $X_i(s)$ are calculated for each of the bins. Finally, k_i and m_i are evaluated by the (best fit) line describing $\ln(\sigma_i(s))$ versus $\ln(\mu_i(s))$; m_i is the slope of this line and $\ln(k_i)$ is its intercept.

Naturally, estimation of k_i and m_i is sensitive to the size of the bins used for sectioning the stimulus range. The bins should be small enough so that the function $\mu_i(s)$ within a given stimulus bin is approximately constant, but also large enough so that a reasonable number of data points is included in each stimulus bin.

2.2.2. Low spike count

To estimate $P_i(s)$ we divide the range of stimulus values into a set of successive bins. The firing probability within each stimulus bin is given by the ratio of the

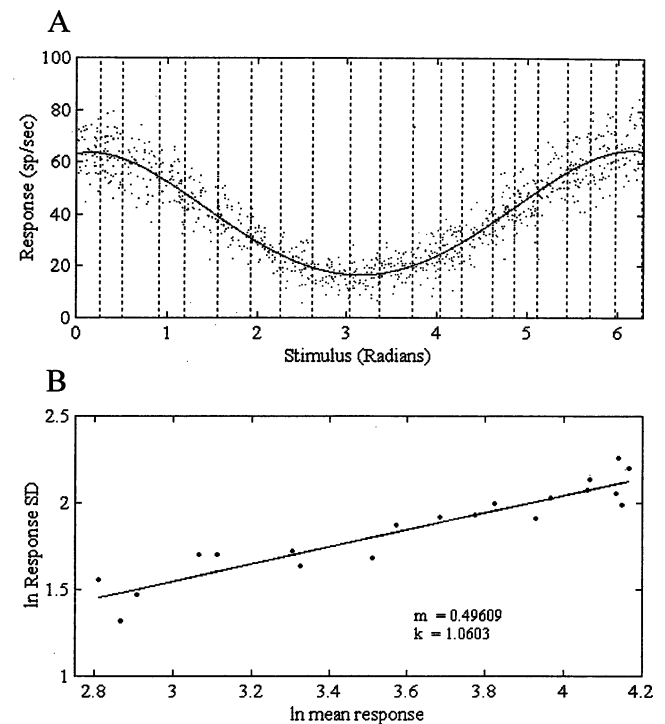


Fig. 1. Estimation of spike count distributions. A: Estimation of mean response function $\mu(s)$ is accomplished by fitting a polynomial (continuous curve) to the spike counts as a function of stimulus value (dots). B: Estimation of the relationship between the standard deviation $\sigma(s)$ and the mean response $\mu(s)$ by the relation $\sigma(s) = k\mu(s)^m$ with m and k constants. The range of stimuli is divided into consecutive bins, as shown by the dotted vertical lines in (A). A line is then fitted to the data points representing natural logarithm (SD) of the counts in each of the stimulus bins vs. the natural logarithm of the average stimulus in that bin. The slope of the line gives m and the intercept gives $\ln(k)$. To generate the data set for this illustration, we simulated the response of a neuron with a normal spike count distribution: $x(s) \sim n(\mu(s), \mu(s)^{0.5})$ with $\mu(s) = 40 + 26 \cos(s)$ sp/s; Thus $k = 1$ and $m = 0.5$. A total of 1000 stimuli s were sampled uniformly from the continuous range $[0, 2\pi]$ radians. The polynomial order used for estimating the mean response in (A) is 4. To estimate k and m the stimulus range was sectioned into 20 bins, each containing 50 responses.

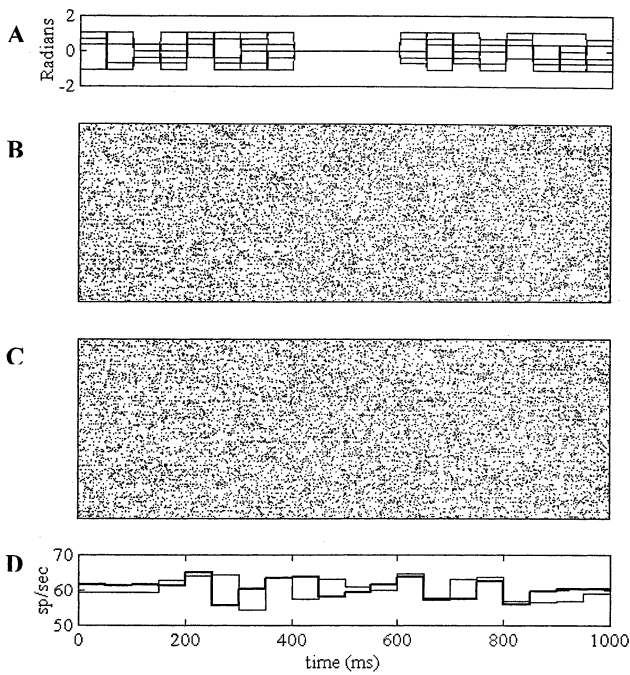


Fig. 2. Simulation of Poisson spike trains during trials with temporally modulated stimulus variability. 200 trials of 1 s each were simulated at 1 ms resolution. Mean response functions for both neurons are $\mu(s) = 60 - 50 \sin(s)$ sp/s. In each 50 ms time interval the stimulus s was randomly selected, separately for each trial, from a discrete uniform distribution with s ranging between $-\pi/3$ and $\pi/3$ at increments of $\pi/9$, except for the time interval 400–600 ms where the value of s was 0 in all trials. A: Examples of stimuli from 8 trials. Note that in the interval 400–600 ms stimulus values are invariably zero. B,C: Dot displays for each of the two neurons. D: PSTHs of both neurons (thin and thick lines) calculated with a 50 ms time bin.

number of trials where a spike occurred (i.e. $X_i(s) = 1$) to the total number of trials in that bin. Finally, $P_i(s)$ is evaluated as the best fit polynomial between the firing probabilities and the stimulus values in each bin. The polynomial order is determined as described in the previous subsection.

3. Results and analysis

3.1. Example: apparent correlations resulting from stimulus variability

In Fig. 2 we show dot displays of simulated spike trains from two neurons for a set of 200 trials. The spike trains were modeled as non-homogenous Poisson processes, with rates, identical for both neurons, given by $\mu(s) = 60 - 50 \sin(s)$ sp/s where s is the stimulus; for example, we may think of s as the orientation of a visual stimulus. We stress that although both neurons are characterized by the same firing rate, the spike trains of the neurons were generated independently. Thus, by construction, any correlation between the

neurons is due to their common mean responses, and not to correlated fluctuations around these means.

To generate the data in Fig. 2, spike trains of 1000 ms duration were simulated at 1 ms resolution, so that, within a given 1 ms time interval, a spike occurred with probability $\mu(s)/1000$. To produce the stimuli, the trial duration was divided into twenty 50 ms bins, within which the stimulus value was kept constant, as shown in Fig. 2A. In one specific time interval (400–600 ms), corresponding to four time bins, the value of s was kept constant ($s = 0$, $\mu(s) = 60$ sp/s) in *all* trials. For all other time intervals, s was randomly selected, separately for each trial, from a discrete uniform distribution with s ranging between $-\pi/3$ and $\pi/3$ at increments of $\pi/9$. A visual examination of the dot displays does not reveal any obvious difference between the 400 and 600 ms time interval and the rest of the trial.

Fig. 3A shows a JPSTH of the spike counts of the two neurons, calculated using a 50×50 ms time bin, normalized so as to give the correlation coefficient within each bin (Aertsen et al., 1989). The time evolving zero lag correlation, as represented by the diagonal bins (Fig. 3C), is nearly zero during the interval 400–600 ms, whereas, outside this interval, it is clearly positive.

In Fig. 3B we see that the JPSTH appears dramatically different if the correlation is calculated using the noise elements $N_i(s)$ (Section 2.2), rather than the spike counts $X_i(s)$. Here we clearly see that the noise correlation is virtually zero throughout the *entire* trial.

This example illustrates how dynamics of interaction may seem to occur, when in fact the spike count correlation reflects only *dynamics of stimulus variability*. In general, the correlation between the $N_i(s)$'s need not

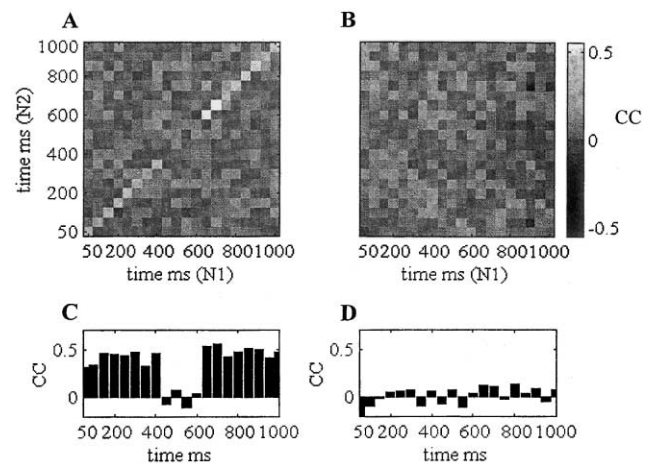


Fig. 3. JPSTHs of the spike trains shown in Fig. 2. A: JPSTH of spike counts. B: JPSTH of noise components $N_i(s)$. C: diagonal bins of spike count JPSTH. D: Diagonal bins of noise JPSTH. Bin size for both JPSTHs is 50×50 ms. Both JPSTHs are normalized so as to give the correlation coefficient of spike counts within each bin. Bar on the right provides the scale for the correlation coefficient within each of the JPSTH bins.

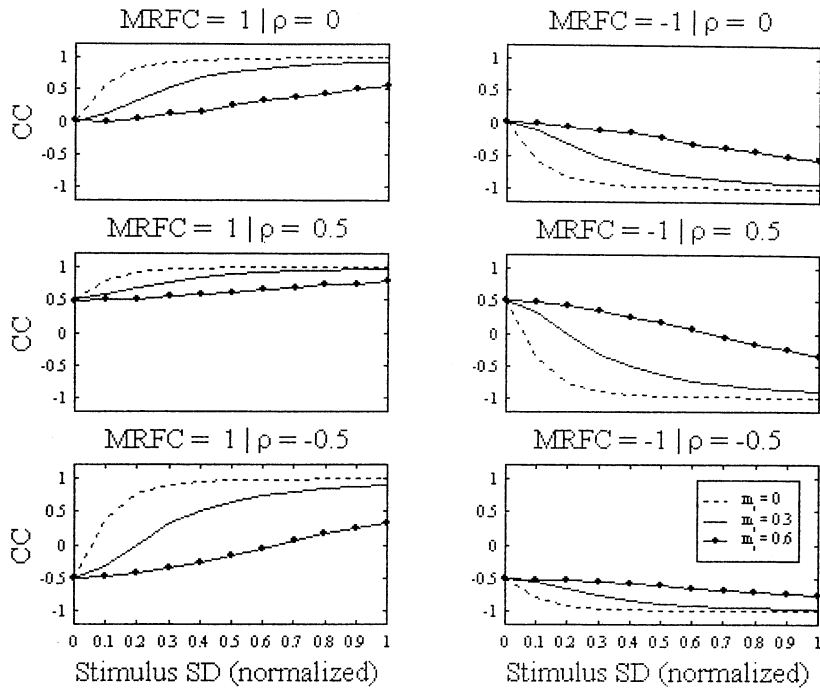


Fig. 4. Spike count correlation as a function of stimulus variability. Each curve shows the correlation coefficient between spike counts of two neurons following bi-normal spike count distributions, with means given by $(\mu_1(s), \mu_2(s))$; standard deviations (SDs) given by $(\mu_1(s)^{m_1}, \mu_2(s)^{m_2})$ and a correlation coefficient (ρ). Left panels: identical response functions for both neurons $\mu(s) = 50 + 40$ s sp/s. Right panels: anti-correlated response functions: $\mu_1(s) = 50 + 40$ s sp/s; $\mu_2(s) = 50 - 40$ s sp/s. Upper panels: ρ (intrinsic correlation) = 0; middle panels: $\rho = 0.5$; bottom panels: $\rho = -0.5$. For each data point, 10 000 stimulus values were sampled from a continuous uniform distribution $u[-\Delta s, \Delta s]$ with Δs ranging between 0 and 0.5, at increments of 0.05. The horizontal axis shows the SD of the stimulus, normalized by the SD at the maximum range of $\Delta s = 0.5$. The three curves in each of the panels correspond to three different values of m_i (identical for both neurons): 0, 0.3 and 0.6.

be zero, in which case, corrections for the dependence of the noise distribution on the mean response are also required. This last issue is discussed in Section 3.2.2 and in Appendix B.

3.2. High spike count

3.2.1. Apparent correlation

In this section we discuss the effect of stimulus variability on the correlation coefficient between spike counts of two neurons in the high count limit. We assume that the standard deviation of the noise depends on the mean response as described in expression (2). Using this assumption, we show in Appendix A that the correlation coefficient between the spike counts of two neurons is given by

$$CC(X_1, X_2) = \frac{\text{cov}(\mu_1(s), \mu_2(s)) + k_1 k_2 \langle \mu_1(s)^{m_1} \mu_2(s)^{m_2} 2\tilde{N}_1 \tilde{N}_2 \rangle_s}{\sqrt{\text{var}(\mu_1(s)) k_1^2 \langle \mu_1(s)^{2m_1} \rangle} \sqrt{\text{var}(\mu_2(s)) + k_2^2 \langle \mu_2(s)^{2m_2} \rangle}} \quad (4)$$

where $\langle \dots \rangle_s$ denotes the expected value for a given value of s , and $\langle \dots \rangle$ denotes the expected value over all values of s . All covariance and variance terms are calculated over all values of s . From this equation it is apparent that the correlation coefficient involves an interplay between the Intrinsic Correlation (IC) and the

stimulus variability. A qualitative understanding of this statement is provided by considering two extreme cases. First, if the stimulus is constant, then all mean response variance and covariance contributions vanish, and (4) reduces to the IC between the neurons, namely

$$CC(X_1, X_2) = \langle \tilde{N}_1 \tilde{N}_2 \rangle \quad (4a)$$

In the other extreme, consider a situation where the spike count variance is 0 for all s , i.e. $k_1 = k_2 = 0$. In this case (4) reduces to

$$CC(X_1, X_2) = \frac{\text{cov}(\mu_1(s), \mu_2(s))}{\sqrt{\text{var}(\mu_1(s))} \sqrt{\text{var}(\mu_2(s))}} \quad (4b)$$

which is the correlation coefficient between the mean response functions over all stimulus values. We shall refer to the right side of (4b) as the mean response function correlation (MRFC).

To gain further insight into the behavior of expression (4) we show in Fig. 4 how the correlation coefficient between spike counts of two neurons is effected by stimulus variability. Each of the six panels in the figure corresponds to a specific combination of IC (given by ρ) and mean response function correlation (MRFC). Within each panel, we show how the spike count correlation behaves as a function of stimulus variability

(horizontal axis), and noise variance (different curves in each panel).

Specifically, spike counts were derived from a joint bi-normal distribution, and are thus characterized by their means and standard deviations, as well as the IC (given by ρ). The three panels on the left display the correlation coefficient between two neurons with identical response functions: $\mu(s) = 50 + 40$ s sp/s (MRFC = 1). The three panels on the right correspond to a pair of neurons with anti-correlated response functions: $\mu_1(s) = 50 + 40$ s sp/s, $\mu_2(s) = 50 - 40$ s sp/s (MRFC = -1). The top, middle, and bottom panels in both columns correspond to three different values of the IC: $\rho = 0, 0.5$, and -0.5 , respectively. In all cases, the standard deviation of the spike counts is given by $\sigma_i(s) = k_i \mu_i(s)^{m_i}$ (expression (2)). The three curves in each of the panels correspond to different values of m_i : 0, 0.3, and 0.6 (identical for both neurons); in all cases $k_i = 1$. Stimulus values were sampled from a continuous uniform distribution $u[-\Delta s, \Delta s]$ with Δs ranging between 0 and 0.5, at increments of 0.05. The horizontal axis shows the normalized SD of the stimulus (i.e. the SD divided by the maximal SD). For each data point (characterized within each panel by a specific combination of Δs and m_i) 10000 stimulus values were sampled.

The quantitative analysis presented here is strictly applicable only for the specific set of conditions described above. Nevertheless, on the basis of the results shown in Fig. 4, two important conclusions are evident, regardless of the details of the spike count distributions and stimulus variability. First, we note that when the stimulus variability approaches zero, the spike count correlation approaches the IC. In contrast, when stimulus variability is large, the spike count correlation approaches the MRFC. In general, the observed correlation coefficient assumes values intermediate between the MRFC and the IC. For example, when the IC and the MRFC are of opposite signs, stimulus variability may result in a spike count correlation of opposite sign to that of the IC (see for example the bottom left or middle right panels in Fig. 4). Second, the smaller the variance of the spike count distribution for a given stimulus value, the faster the approach of the spike count correlation to the MRFC limit with increasing stimulus variability. In Fig. 4 we have explicitly considered only variations in m (expression (2)). However, similar behavior results from variation in k . Namely, a smaller value of k implies a faster approach of the spike count correlation to the MRFC limit.

3.2.2. Evaluating the intrinsic correlation

To eliminate the effect of stimulus variability on the spike count correlation, the noise elements, rather than the spike counts must be correlated. If the noise elements of both neurons are independent, the IC and the noise correlation are both equal to zero. However, if

the noise elements are correlated, and if the noise distributions depend on the stimulus value, then stimulus variability will also be reflected in the noise correlation, as explained in Appendix B. To correct for this effect, several assumptions regarding the dependence of the noise on the stimulus are necessary. Specifically, assuming the dependence of $\sigma_i(s)$ on $\mu_i(s)$ as given in expression (2), we evaluate the normalized noise elements \tilde{N}_i (Section 2.2), and correlate them to obtain the IC. Standard statistical tests can then be used to set confidence intervals on the observed ICs (Sokal and Rohlf, 1995).

Finally, if the IC is a function of the stimulus, and if the stimuli vary from trial to trial, then the observed IC reflects an average of the IC over stimulus values in each of the trials. This is a critical point as it implies that in general, in order to study the relationship between stimulus and IC, it is required to maintain the stimulus constant. Nevertheless, if the IC is approximately a linear function of the stimulus (within the relevant range of stimulus values) then the observed IC provides a good approximation to the IC for the average stimulus value.

3.3. Low spike count

3.3.1. Expected coincidences

As described in Section 2.1.2, when the spiking probabilities of both neurons, P_1 and P_2 are constant and independent, the distribution of coincidences (Z) is given by binomial ($P_1 P_2 n$), where n is the number of trials. Here, we will use $P_i(s_j)$ to denote the firing probability of neuron i in response to s_j , the stimulus value in trial j . The coincidence probability of neurons $i = 1$ and 2 in trial j is given by $Q_j = P_1(s_j)P_2(s_j)$. The probability of observing z coincidences in n trials is given by

$$P(Z = z) = \sum_{V \in V_{nz}} \prod_{j=1}^n Q_j^{V_j} (1 - Q_j)^{(1 - V_j)}. \quad (5)$$

In this equation V_{nz} is the set of all vectors with n elements ($v_1, v_2, \dots, v_j, v_n$) so that z of the elements are equal to 1, and the rest of the elements are equal to 0. Thus, each vector $V \in V_{nz}$ describes an event (i.e. a sequence of trials), in which a coincidence occurred in z trials, and no coincidence occurred in the rest (i.e. in $n-z$) of the trials. The probability of observing the event denoted by V is given by the product in (5). Unlike the case of a binomial distribution where all events $V \in V_{nz}$ are equally likely, here each of these events is associated with a different probability. The sum in (5) is over all events in which exactly z coincidences occurred. For a large n , and different Q_j 's for different trials, the calculation of (5) is impractical. Fortunately, in this limit the normal distribution provides a good approximation for the probability distribution of z , namely $Z \sim$

$n(E(Z), \sigma(Z))$ (Feller, 1966, see also Baker et al., 2001). Since the coincidences in each trial are independent of each other, we have $E(Z) = \sum Q_j$ and $\sigma^2(Z) = \sum Q_j(1 - Q_j)$ where the sums are over the trial index j .

To demonstrate the effect of a variable firing probability (resulting from varying stimuli), we display in Fig. 5 the exact and the normal approximations for the distribution of Z under several conditions. Fig. 5A shows the probability distribution of Z for a set of 100 trials for two neurons with identical firing probabilities (MRFC = 1). In 50 of the trials, the firing probabilities of both neurons in each bin are given by $0.3 - \Delta$, and in the other 50 trials, by $0.3 + \Delta$. The three staircase curves correspond to $\Delta = 0, 0.1$, and 0.2 . For example, the leftmost curve ($\Delta = 0$) is for the case where the firing probabilities are 0.3 for both neurons on all trials; only in this case is the distribution of z truly binomial. The other staircase curves ($\Delta = 0.1$ and $\Delta = 0.2$) represent increasing firing probability variability. On each of the curves we superimposed the corresponding normal approximations. The important feature of the curves in Fig. 5A is that upon increasing firing probability variability, the probability distributions of Z shift to the right. Another way of representing the same data is shown in Fig. 5C where the probability of obtaining a

coincidence value higher than or equal to z is plotted. This representation shows that *high* values of Z become increasingly likely upon an increase in the firing probability variability.

Fig. 5B shows the distributions of Z when the firing probabilities of both neurons are anti-correlated (MRFC = -1). Specifically, in 50 trials the firing probabilities are $0.3 - \Delta$ for one neuron, and $0.3 + \Delta$ for the other. In the other 50 trials, the firing probability of one neuron is $0.3 + \Delta$, and $0.3 - \Delta$ for the other neuron. Again, the three pairs of curves correspond to $\Delta = 0, 0.1$, and 0.2 . Here, the *rightmost* curves correspond to the binomial distribution, and as the firing probability variability is increased the curves shift to the *left*. Fig. 5D shows the cumulative distributions of Z , i.e. the probability to obtain a value of the coincidence equal to or lower than z . In this case, *low* values of Z are more likely when the firing probability variability is increased.

Thus, as trial to trial stimulus variability is increased, it is increasingly likely to reject the ‘null hypothesis’ of independence between the neurons when the assumption of ‘no trial to trial stimulus variability’ is implicitly made. When the assumption of ‘no trial to trial stimulus variability’ is not warranted, the proper test for

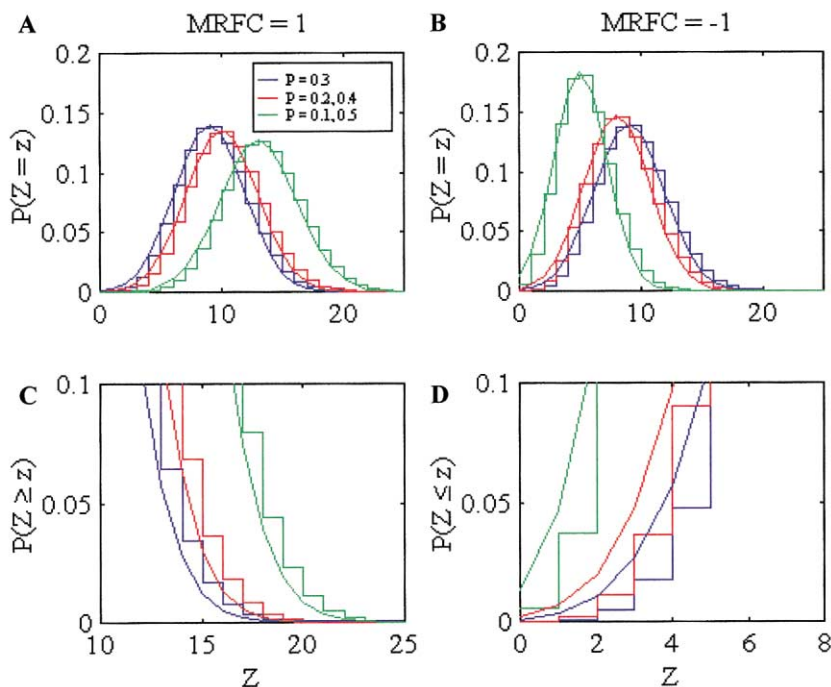


Fig. 5. Exact and normal approximations for the distribution of coincidences (Z) under several conditions. A: Probability distribution of Z in 100 trials for two neurons with identical firing probabilities. In 50 of the trials, the firing probabilities of both neurons in each bin are given by $0.3 - \Delta$, and in the other 50 trials, by $0.3 + \Delta$. The three staircase curves correspond to $\Delta = 0, 0.1$, and 0.2 . On each of the staircase curves are superimposed the corresponding normal approximations. B: Same as A except that here the firing probabilities of both neurons are *anti-correlated*. Specifically, in 50 trials the firing probabilities are $0.3 - \Delta$ for one neuron, and $0.3 + \Delta$ for the other. In the other 50 trials, the firing probabilities of one neuron are $0.3 + \Delta$, and $0.3 - \Delta$ for the other neuron. C: $P(Z \geq z)$ for the probability distributions in (A). Only high values of Z are plotted in order to highlight ‘extreme’ values of z . D: $P(Z \leq z)$ for the probability distributions in (B). Only low values of Z are plotted. Although the probability distributions are defined only for integer values of Z , they were plotted as continuous curves for clarity.

independence should involve comparison of the observed value of Z to its expected distribution given the stimulus values in each of the trials, as described above.

3.4. Predictions regarding the apparent dependence of correlation on stimulus

In the previous sections we have considered correlations between a pair of neurons characterized by a fixed relationship between their mean response functions. In the more general (and realistic) case, neurons may have different and non-linear response functions over the stimulus range. In such a situation, the correlation between the response functions of both neurons is different for different stimulus values. By considering the neuronal response functions and the stimulus variability it is possible to predict the patterns of correlations as a function of the stimulus value.

Let us consider two independent neurons ($IC = 0$), $i = 1, 2$ with mean response functions $\mu_i(\theta, v) = A_i + vB_i \cos(\theta - \theta_i)$ sp/s where θ and v are random variables characterizing the stimulus, and θ_i , A_i and B_i are constants. Note that here the stimulus is two dimensional, $s = [\theta, v]$. The spike counts of the neurons are normally distributed with $n(\mu_i(\theta, v), \sigma_i(\theta, v))$. Furthermore, following expression (2) we again use $\sigma_i(\theta, v) = k_i \mu_i(\theta, v)^{m_i}$, with m_i and k_i constants. Such response functions may describe arm related motor neurons in M1 with mean responses that are tuned to direction θ_i and scaled by the velocity v ; alternatively θ_i and v may be interpreted as the orientation and the contrast of a visual stimulus.

Consider now a trial which requires a hand movement to direction θ_n (the ‘intended’ direction) performed with velocity v . Suppose that upon each repetition of the trial, the direction of motion deviates from θ_n by $\Delta\theta_n$, with a different $\Delta\theta_n$ for different trials. If, around θ_n , the slopes of the mean response functions (μ_1, μ_2) with respect to θ are of opposite sign, then random deviations from θ_n will cause negative correlations. In contrast, if the slopes are of similar sign, then variations in direction will induce positive correlations. The exact magnitude and sign of the correlations, for each given direction θ_n , are a function of $\Delta\theta_n$ (i.e. the variability of movement direction in that specific direction) as well as the ratio of the slopes of the two response functions at θ_n . Movements may also vary in velocity but not in direction. In this case, stimulus related correlation still occurs, but its sign and magnitude are determined by the derivatives of the response functions with respect to the velocity (v) rather than direction (θ).

To illustrate these points, we have simulated the responses of two neurons, with response functions of the form given above, using $A = 50$ sp/s, $B = 40$ sp/s, $k = 1$, $m = 0.3$, $\theta_1 = 0$, $\theta_2 = 1$ radian, and intended directions θ_n in the range $[0, \Pi]$ radians (sampled in steps

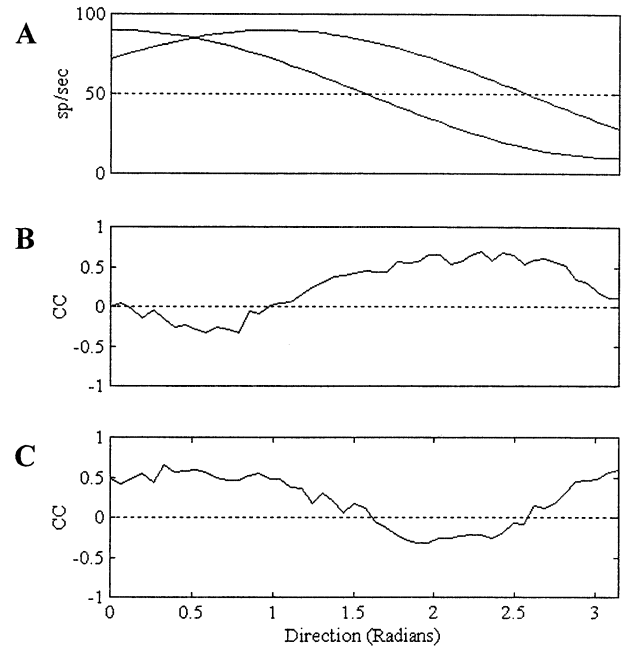


Fig. 6. Tuning of spike count correlation as a result of stimulus variability. Simulation of two independent neurons with normal spike count distributions: $n(\mu_i(\theta, v), \mu_i(\theta, v)^{0.3})$ where $\mu_1(\theta, v) = 40 + v50 \cos(\theta)$ sp/s and $\mu_2(\theta, v) = 40 + v50 \cos(\theta - 1)$ sp/s; θ is specified in radians. A: Response functions of both neurons as a function of θ for $v = 1$. B: Correlation coefficient between the spike counts as a function of intended direction θ_n with variable directions in each trial. For each intended direction θ_n , the actual directions were randomly selected from a uniform distribution in the range $[\theta_n - 0.2, \theta_n + 0.2]$ radians. The value of v was set at 1 for all intended directions. C: Correlation coefficient between the spike counts as a function of intended direction θ_n with variable velocities in each trial. For each intended direction, v was uniformly sampled from the continuous range $[0.8, 1.2]$, whereas the directions were set constant at θ_n . In both cases, 200 trials were simulated for each intended direction θ_n . The intended directions were obtained from the range $[0, \Pi]$, sampled in steps of 0.0654 radians.

of 0.0654 radians). The response functions of both neurons are shown in Fig. 6A as a function of θ_n for $v = 1$. Simulating the responses of both neurons in 200 trials, we calculated the correlation coefficient between the spike counts over a 1 s time interval as a function of θ_n .

In the first simulation, we simulated responses to variable directions (Fig. 6B). That is, each point on the θ axis corresponds to an intended direction θ_n , with directions randomly selected from a continuous uniform distribution in the range $[\theta_n - 0.2, \theta_n + 0.2]$ radians. The value of v was set at 1 for all intended directions. The curve in Fig. 6B shows the correlation coefficient of the simulated responses as a function of the intended movement direction θ_n . In the second simulation, velocities (but not directions) varied from trial to trial. In each intended direction, v has been uniformly sampled from the continuous range $[0.8, 1.2]$, while the directions were set constant at θ_n . The curve

in Fig. 6C shows the correlation coefficient between the simulated spike counts. Examination of the correlations in Fig. 6B and 6C shows that the sign of the correlations is determined, as expected, by the product of the derivatives of the response functions with respect to direction and velocity, respectively.

Of course, more complex patterns of correlation as a function of stimulus value are expected when both directions and velocities, and possibly other parameters, vary from one trial to another. In addition, in these simulations, the stimulus variability (in either θ or v) was identical for all intended directions θ_n . Had the variability been different for different θ_n , we would observe more complex relationships between the correlation and the stimulus.

4. Discussion

In this report we have argued that stimulus variability can cause apparent neuronal correlation or synchrony. The main goal of our analysis has been to describe the qualitative, rather than the quantitative, effects of stimulus variability on the observed spike count correlation. To demonstrate the possible outcomes of stimulus variability, we considered simulated data sets (Section 3.1 and Section 3.4) with quite large, yet not unrealistic, stimulus variability. The dependence of the observed correlation on the magnitude of stimulus variability was studied in further detail in Sections 3.2. and 3.3. In general, the applicability of our conclusions to any given data set depends on the exact form of the spike count distributions, as well as the stimulus values in each of the trials.

4.1. Related previous studies

The dangers associated with the implicit assumption of various physiological studies according to which all trials are identical, has already been addressed by (Brody, 1999a,b). In these reports Brody points out two possible scenarios which can result in effects similar to those described here. Namely, it has been shown that co-variations of either neuronal excitability (on a slow time-scale, i.e. approximately constant excitability during a single trial) or of response latency, can result in artifactual spike count correlations. In the present report however, the focus is on one common mechanism, namely stimulus variability, which can account for such trial to trial variability. We have attempted to show that changes in trial to trial variability (either in the course of time within a trial, and/or across different conditions) may assume various forms, each associated with a different pattern of the resulting spike count correlations. Focusing on a specific mechanism, we were able to suggest methods to eliminate the effects of

trial to trial variability. Although the effects mentioned here are not likely to be expressed as slow time scaled excitability changes, they may well result in variations in latency of neuronal response, as described by Brody. In this respect Brody's approach and ours are complementary.

In Section 3.4 we have shown how stimulus variability may account for apparent stimulus dependent correlations. Theoretical accounts of stimulus dependent correlations and their dependence on neuronal tuning functions have already been described by others (Ben-Yishai et al., 1994; Pouget et al., 1998). However, while in those reports correlations were shown to result from properties of the network architecture, our arguments imply that stimulus dependent correlations may occur without any direct connectivity between neurons.

4.2. Assumptions regarding the neuronal response functions

To demonstrate how the intrinsic correlation can be evaluated from spike counts and the stimulus values, we have used rather simple neuronal response functions (Section 2.2). Specifically, we have assumed that neuronal responses can be described as step functions with zero temporal delay following stimulus presentation. In reality, neuronal response functions are more complex. Responses to a given stimulus are generally dynamic, the responses to a sequence or a combination of stimuli is in general not a linear sum of the responses to each of the single stimuli, and time delays not only exist, but may also depend on the value of the stimulus (Schwartz, 1994). Therefore, our proposed method for estimating the neuronal response functions should be regarded as a first approximation. Whether this first approximation is adequate depends on the actual (unknown) response functions. Since sample sizes (i.e. number of trial repetitions) are typically limited, and the dependence of neuronal response functions on multi-dimensional stimulus values is complex, it seems hard, if not impossible, to obtain these functions exactly. Nevertheless, we believe that application of even the simple methods suggested here, to various candidate stimuli (i.e. to all stimuli recorded during an experiment) can advance the goal of disambiguating the IC from that caused by stimulus variability.

4.3. Implications for designing and interpreting experiments

It is obviously preferable to record as many stimuli/actions as possible, thus increasing the reliability of the estimates of the neuronal response functions. During trial performance however, it is critical to minimize the variability of all stimulus and action dimensions to which the neurons may respond. While this goal can never be fully attained, it should always be pursued.

Suppose that after taking into account the variability of all stimuli and actions recorded during an experiment, nonzero IC still prevails. Suppose also that the observed IC is modulated as a function of time or of the behavioral condition. What do these correlations actually reflect? We can think of two possible scenarios regarding the nature of the correlations. In the first, the *causal* scenario, the activity of one of the neurons (or both) is effecting the activity of the other. These could occur via direct synaptic interactions, or by one or more intermediate relaying neurons. Such an interaction could only be confirmed (or refuted) if a test of causality between the activities of both neurons is performed.

In the second scenario, it is a *common source* which affects both neurons, so that no causal relationship exists between the neurons. Naturally, the inputs from this common source must vary in order to induce correlation between the neurons. The interesting question which then remains concerns the nature of the common source. Specifically, it may be the variability of some stimulus or action not recorded during the experiment that is responsible for the observed correlation. Only if there is a good reason to believe that the variability of all relevant stimuli or actions has been accounted for, are we in a position to conclude that it is some *internal variable* (i.e. not a sensory input or a motor output) whose variability induces the correlations.

4.4. Generalization

Throughout this paper we have considered a situation where two neurons are responsive to a common stimulus. However, other scenarios where stimulus variability may play a role occur when the two neurons are related to different stimuli, and these stimuli are differentially correlated with each other in different contexts. To illustrate, consider two neurons, each of which is associated with a single muscle. Now, consider two actions, one which demands coordination between the muscles, so that their activities are correlated, and another which does not require coordination, so that the muscles are not correlated. If upon repetitions of each of the actions, the muscle activities vary, correlations between the neuronal activities would appear during the first action, but not during the second. In the first action, where both muscles are correlated, they are functionally equivalent to a single stimulus effecting both neurons. In the second action, the muscles are not correlated, and therefore no common stimulus effects both neurons. In this example, then, it is not the variability of a single stimulus, but rather the covariance of two stimuli which must be considered. Phrased more generally, any interpretation of neuronal correlations must take into account the statistics of all the stimuli to which the neurons are related.

To summarize, our central claim is that while changes in correlations might reflect changes in direct (causal) interactions between neurons, they may also reflect the individual response properties of neurons to varying stimuli. While this view may seem pessimistic, the situation is not as hopeless as it might seem: If the variability of all stimuli to which the neurons in question are known to respond have been accounted for, and if correlations still remain, then either: (1) The correlations reflect a causal interaction between the neurons, or (2) The correlations result from variability of some common stimulus which is not known to influence the neurons. Whichever of the above is the case, the observed correlation reflects something beyond what is known about the neuronal response functions and are therefore interesting.

Acknowledgements

This study was supported in part by the Israeli Academy of Sciences and the US-Israel Bi-national Science Foundation. We thank David Arkadir and Genella Morris whose results and preliminary analysis motivated this work. We thank Ad Aertsen and Felix Kuemmelman for providing us with the JPSTH software they developed and Eilon Vaadia for his comments on early versions of the manuscript. Special thanks are due to Avinoam Ben-Shaul for valuable insights and suggestions.

Appendix A. Spike count correlation in the high count limit

From the description of X_i in expression (1) it follows that the correlation coefficient between the spike counts of two neurons (1 and 2) is given by

$$CC(X_1 X_2) = \frac{\text{cov}(\mu_1 + N_1, \mu_2 + N_2)}{\sqrt{\text{var}(\mu_1 + N_1)}\sqrt{\text{var}(\mu_2 + N_2)}} \quad (\text{A1})$$

$$= \frac{\text{cov}(\mu_1, \mu_2) + \text{cov}(\mu_1, N_2) + \text{cov}(\mu_2, N_1) + \text{cov}(N_1, N_2)}{\sqrt{\text{var}(\mu_1 + N_1)}\sqrt{\text{var}(\mu_2 + N_2)}}$$

where in the second equality we have used the identity $\text{cov}(A + B, C + D) = \text{cov}(A, C) + \text{cov}(A, D) + \text{cov}(B, C) + \text{cov}(B, D)$ with A , B , C , and D any random variables. Recall that for any random variables A , B , and C

$$\text{cov}(A, B) = \langle \text{cov}(A, B|C) \rangle + \text{cov}(\langle A|C \rangle, \langle B|C \rangle). \quad (\text{A2})$$

Here $\langle A|C \rangle$ is the expected value of A for a given value C , and $\langle \text{cov}(A, B|C) \rangle$ is the expected value of the covariance of A and B over all values of C . Similarly, $\text{cov}(\langle A|C \rangle, \langle B|C \rangle)$ denotes the covariance of A and B , given C , over all values of C . Using (A2), and since the

expected value of $N_i(s)$ is, by definition, zero for any value of s , we obtain for all combinations of $i = 1, 2$ and $j = 1, 2$

$$\text{cov}(\mu_i, N_j) = \langle \text{cov}(\mu_i(s), N_j(s)) \rangle + \text{cov}\langle \mu_i(s), 0 \rangle = 0 \quad (\text{A3})$$

so that the two middle terms in the numerator of A1 vanish. Also, from (A3): $\text{var}(\mu_i + N_j) = \text{var}(\mu_i) + \text{var}(N_j) + 2\text{cov}(\mu_i, N_j) = \text{var}(\mu_i) + \text{var}(N_j)$. Hence, (A1) becomes

$$CC(X_1, X_2) = \frac{\text{cov}(\mu_1, \mu_2) + \text{cov}(N_1, N_2)}{\sqrt{\text{var}(\mu_1) + \text{var}(N_1)}\sqrt{\text{var}(\mu_2) + \text{var}(N_2)}} \quad (\text{A4})$$

Our next step is to express the N_i 's in terms of the normalized noise \tilde{N}_i , as given by expression (2). To express the variance of N_i note that by substituting (2) into (A4) and recalling that $\text{var}(A) = \langle \text{var}(A|C) \rangle + \text{var}\langle A|C \rangle$ we find

$$\begin{aligned} \text{var}(N_i) &= \langle \text{var}(N_i|s) \rangle + \text{var}\langle N_i|s \rangle = \langle \sigma_i^2(s) \rangle + \text{var}(0) \\ &= k_i^2 \langle \mu_i(s)^{2m_i} \rangle. \end{aligned} \quad (\text{A5})$$

To express the covariance of N_1 and N_2 in terms of the normalized noise we use (A2), finding

$$\begin{aligned} \text{cov}(N_1, N_2) &= \langle \text{cov}(N_1, N_2|s) \rangle + \text{cov}(0, 0) \\ &= \langle \text{cov}(k_1\mu_1(s)^{m_1}\tilde{N}_1, k_2\mu_2(s)^{m_2}\tilde{N}_2) \rangle \\ &= k_1k_2 \langle \langle \mu_1(s)^{m_1}\tilde{N}_1\mu_2(s)^{m_2}\tilde{N}_2 \rangle_s \rangle \end{aligned} \quad (\text{A6})$$

where the inner brackets $\langle \dots \rangle_s$ denote the expected value for a given value of s , and the outer brackets $\langle \dots \rangle$ denote the expected value over all values of s . Next, we apply (A2) to μ_1 and μ_2 , obtaining

$$\begin{aligned} \text{cov}(\mu_1, \mu_2) &= \langle \text{cov}(\mu_1, \mu_2|s) \rangle + \text{cov}(\langle \mu_1|s \rangle, \langle \mu_2|s \rangle) \\ &= \text{cov}(\mu_1(s), \mu_2(s)). \end{aligned} \quad (\text{A7})$$

Finally, we substitute (A5), (A6) and (A7) into (A4) to obtain:

$$CC(X_1, X_2) = \frac{\text{cov}(\mu_1(s), \mu_2(s)) + k_1k_2 \langle \langle \mu_1(s)^{m_1}\mu_2(s)^{m_2}\tilde{N}_1\tilde{N}_2 \rangle_s \rangle}{\sqrt{\text{var}(\mu_1(s)) + k_1^2 \langle \mu_1(s)^{2m_1} \rangle} \sqrt{\text{var}(\mu_2(s)) + k_2^2 \langle \mu_2(s)^{2m_2} \rangle}}$$

Appendix B. Effect of stimulus variability on noise correlation

The correlation coefficient between the noise elements is given by:

$$CC(N_1, N_2) = \frac{\text{cov}(N_1, N_2)}{\sqrt{\text{var}(N_1)}\sqrt{\text{var}(N_2)}}$$

Substituting (A5) and (A6) for the noise variance and covariance, respectively, we obtain:

$$CC(N_1, N_2) = \frac{k_1k_2 \langle \langle \mu_1(s)^{m_1}\tilde{N}_1\mu_2(s)^{m_2}\tilde{N}_2 \rangle_s \rangle}{\sqrt{k_1^2 \langle \mu_1(s)^{2m_1} \rangle} \sqrt{k_2^2 \langle \mu_2(s)^{2m_2} \rangle}}$$

$$= \frac{\langle \langle \mu_1(s)^{m_1}\tilde{N}_1\mu_2(s)^{m_2}\tilde{N}_2 \rangle_s \rangle}{\sqrt{\langle \mu_1(s)^{2m_1} \rangle} \sqrt{\langle \mu_2(s)^{2m_2} \rangle}}$$

If the IC, $\langle \tilde{N}_1\tilde{N}_2 \rangle$, is independent of stimulus value then

$$\begin{aligned} CC(N_1, N_2) &= \frac{\langle \mu_1(s)^{m_1}\mu_2(s)^{m_2} \rangle}{\sqrt{\langle \mu_1(s)^{2m_1} \rangle} \sqrt{\langle \mu_2(s)^{2m_2} \rangle}} \langle \tilde{N}_1\tilde{N}_2 \rangle \\ &= \alpha \langle \tilde{N}_1\tilde{N}_2 \rangle \end{aligned}$$

where the second equality serves to define the 'scale factor' α . Note that all expected values involving $\mu_i(s)$ elements are calculated over *all* values of s , whereas $\langle \tilde{N}_1\tilde{N}_2 \rangle$ denotes the expected value for *any* value of s . The maximal value of α is 1 (when $\mu_1(s)^{m_1} = C\mu_2(s)^{m_2}$ for some constant C) and its minimal value is 0. Thus, the IC is an *upper bound* to the noise correlation. Only when $\alpha = 1$, and/or $\langle \tilde{N}_1\tilde{N}_2 \rangle = 0$, are the IC and the noise correlation identical.

References

- Abeles M. Local Cortical Circuits. Berlin, Heidelberg, New York: Springer-Verlag, 1982.
- Aertsen AM, Gerstein GL, Habib MK, Palm G. Dynamics of neuronal firing correlation: modulation of 'effective connectivity'. J Neurophysiol 1989;61:900–17.
- Baker SN, Spinks R, Jackson A, Lemon RN. Synchronization in monkey motor cortex during a precision grip task. I. Task-dependent modulation in single-unit synchrony. J Neurophysiol 2001;85:869–85.
- Barlow HB. Single cells versus neuronal assemblies. In: Aertsen A, Braitenberg VB, editors. Information Processing in the Cortex: Experiments and Theory. Berlin Heidelberg: Springer-Verlag, 1992:169–74.
- Ben-Yishai R, Lev Bar-Or R, Sompolinsky H. Theory of orientation tuning in visual cortex, Proc. Natl. Acad. Sci. USA, 1994.
- Brody CD. Correlations without synchrony. Neural Comput 1999a;11:1537–51.
- Brody CD. Disambiguating different covariation types. Neural Comput 1999b;11:1527–35.
- Feller W. An Introduction to Probability Theory and its Applications, Volume 2. New York, London: Wiley, 1966.
- Gerstein GL, Bedenbaugh P, Aertsen MH. Neuronal assemblies. IEEE Trans Biomed Eng 1989;36:4–14.
- Gerstein GL, Perkel DH, Subramanian KN. Identification of functionally related neural assemblies. Brain Res 1978;140:43–62.
- Gruen S. Unitary Joint-Events in Multiple-Neuron Spiking Activity: Detection, Significance, and Interpretation. Thun, Frankfurt/Main: Harri Deutsch Verlag, 1996.
- Gur M, Beylin A, Snodderly M. Response variability of neurons in primary visual Cortex (V1) of alert Monkeys. J Neuro 1997;17:2914–20.
- Hatsopoulos NG, Ojakangas C, Paninski L, Donoghue JP. Information about movement direction obtained from synchronous activity of motor cortical neurons. Proc Natl Acad Sci USA 1998;95:15706–11.
- Hebb DO. The Organization of Behavior. New York: Wiley, 1949.
- Ito H, Tsuji S. Model dependence in quantification of spike interdependence by joint peri-stimulus time histogram. Neural Comput 2000;12:195–217.

- Lee D, Port NL, Kruse W, Georgopoulos AP. Variability and correlated noise in the discharge of neurons in motor and parietal areas of the primate cortex. *J Neurosci* 1998;18:1161–70.
- Nicolelis MA, Fanselow EE, Ghazanfar AA. Hebb's dream: the resurgence of cell assemblies. *Neuron* 1997;19:219–21.
- Palm G, Aertsen AM, Gerstein GL. On the significance of correlations among neuronal spike trains. *Biol Cybern* 1988;59:1–11.
- Pouget A, Zhang K, Deneve S, Latham PE. Statistically efficient estimation using population coding. *Neural Comput* 1998;10:373–401.
- Rieke F, Warner C, de Saint Martin A, de Ruyter van Steveninck R, Bialek W. *Spikes*. Cambridge, MA: The MIT Press, 1997.
- Schwartz AB. Direct cortical representation of drawing. *Science* 1994;265:540–2.
- Sokal RR, Rohlf FJ. *Biometry*, 3rd edn, 1995.
- Steinmetz PN, Roy A, Fitzgerald PJ, Hsiao SS, Johnson KO, Niebur E. Attention modulates synchronized neuronal firing in primate somatosensory cortex. *Nature* 2000;404:187–90.
- Turner RS, Owens JWM, Anderson ME. Directional variation in spatial and temporal characteristics of limb movements made by monkeys in a two-dimensional work space. *J Neurophys* 1995;74:684–97.
- Vaadia E, Ahissar E, Bergman H, Lavner Y. Correlated activity of neurons: a neural code for higher brain functions? In: Kruger J, editor. *Neuronal Cooperativity*. Berlin: Springer-Verlag, 1991:249–79.
- Vaadia E, Haalman I, Abeles M, Bergman H, Prut Y, Slovin H, Aertsen A. Dynamics of neuronal interactions in monkey cortex in relation to behavioral events. *Nature* 1995;373:515–8.